Influence of pigment-protein coupling on excitation energy transfer in FMO complex

Davinder Singh[1, a)] and Shubhrangshu Dasgupta[1]
Department of Physics, Indian Institute of Technology Ropar, Rupnagar, Punjab - 140001, India

(Dated: 5 October 2016)

To explain experimentally observed oscillatory dynamics of highly efficient process of excitation energy transfer (EET) in Fenna-Matthews-Olson (FMO) complex, most theoretical models assume the same local protein environment around all the bacteriochlorophyll-a (BChla) sites, contradictory to the structural analysis of FMO complex. Using different values of pigment-protein couplings for different BChla sites, measured in the *adiabatic limit* of electron transfer, we theoretically investigate the effect of inhomogeneous local protein environment on excitation energy transfer. By employing non-Markovian master equation we demonstrate that the asymmetric system-bath coupling leads to the results consistent with the experimental observations. Quantum dynamical simulation suggests that the correlated fluctuations preserve the oscillation of excitation for long time-scales. Further different BChla sites have asymmetric time-scales of oscillations of excitation due to in-homogeneous pigment-protein couplings also.

PACS numbers: 82.20Wt, 82.20Rp, 82.53Ps, 87.15H-
Keywords: Excitation energy transfer, Pigment-protein coupling

I. INTRODUCTION

Photosynthesis is the basic energy source for living organism on this planet, with extremely interesting secretive functionality. Through a number of different physiochemical mechanisms, it harvests the solar energy to produce the biomass for living organism using carbon dioxide and water[1,2]. During photosynthesis, solar photons are first absorbed at the antenna by one of the pigment of light harvesting complex. Thereafter, solar energy is transferred through a series of pigments in the form of their electronic excitation energy to the reaction centre, where the relevant chemical reaction takes place. Although the detailed dynamics of the initial stages of the photosynthesis is still unknown, it promises the solution to renewable energy needs of future[3–8].

Light-harvesting complexes (LHCs) which contain several light absorbing molecules called chromophores have attracted much research interest in recent times[9–12]. One of such complexes, the Fenna-Matthews-Olson (FMO) complex[13], is a trimeric light harvesting complex, with each monomer containing seven bacteriochlorophyll-a (BChla) pigments nested within β-sheets and α-helices from protein[9,14–16]. Recent attraction towards the FMO complex is due to the observation of quantum characteristics in the dynamics of this complex. Through two-dimensional Fourier transform electronic spectroscopy[17,18], a wave-like electronic excitation energy transfer (EET) in this complex is observed, that is originally explained as a reminiscent of quantum coherence in the complex[19,20]. Time scale for which these oscillations persist, is a significant fraction of the total transport time of EET in FMO. It implies that the transport of excitation energy through the FMO complex is a coherent phenomenon, and the EET should not be considered as an incoherent hopping[9].

The EET in photosynthetic complexes is mainly characterized by three different parameters[21]: (a) BChla site energies: although chemical composition of all the seven BChla of the FMO complex is the same, due to different protein environment of each BChla site, their site energies are different[22]. (b) Pigment-pigment coupling: this represents the Coulomb interaction between two BChla sites in the dielectric environment[22]. (c) Pigment-protein coupling: this is the coupling between the BChla site and its protein environment. In many of the previous studies[23–46] to understand the oscillatory dynamics of EET in FMO complex, the third parameter is often overlooked. It must be noted that the dissipation rate due to environment is a function the pigment-protein coupling and is relevant to the efficiency of EET in FMO complex. Moreover, the dephasing or decoherence of the BChla sites is important to consider, that also depends upon this coupling. Therefore, careful treatment for pigment-protein coupling is warranted in order to mimic the realistic protein environment for each BChla site.

In the previous theoretical reports[23–46], the local environment of each Bchla site in FMO complex is assumed to be the same. Hence, the coupling of all the different BChla sites with the protein environment is considered to be identical. But there are significant local differences in the protein structure around each BChla site[9,47]. For example, the protein around the BChla 2 is open to the solvent and central Mg atom of BChla 2 has strong coordination with water molecule, while in the opposite case, the BChla 7 is buried deeply in the protein and its Mg atom has poor coordination with surrounding. Now the BChla 2, which lies at protein solvent interface, have

a)Electronic mail: davinder.singh@iitrpr.ac.in

strong interaction (hence strong coupling) with the environment due to solvating water molecule as compared to the BChla 7, which lies deep inside the protein. It implies that the pigment-protein couplings of all the different BChla site in FMO complex must be different.

In this paper, we consider the effect of site-specific pigment-protein couplings on the EET in the *aidiabatic limit*. In this limit, the time-scale t_{el} of electronic wave function to move from the donor BChla site to a degenerate acceptor BChla site is much less than the characteristic time-scale t_{vib} for vibrational motion[21]. We use these different values of pigment-protein couplings to explore how the local differences in the protein structure around each BChla site affect the energy transfer in this complex.

This paper is organized as follow: In section II we introduce the Hamiltonian used to describe the FMO complex and the relevant non-Markovian master equation. Next in section III, we present the solution of this equation and compare the results for different sets of interaction strengths. Finally we conclude the paper in section IV.

II. MODEL

To describe the EET in FMO complex, each jth BChla site is modelled as a two-level system with relevant energy levels $|e_j\rangle$ and $|g_j\rangle$ as illustrated in figure 1. In FMO

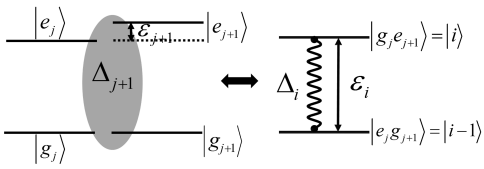

FIG. 1: The schematic on left illustrates the interaction of two BChla sites. On the right is the effective two-level system formed from a pair of interacting BChla sites.

complex, to check the dynamics of EET only, the single excited state is accountable[43,48]. In this effective site-basis, the total Hamiltonian can be written as

$$H = H_S + H_B + H_{SB} \ , \tag{1}$$

where the system Hamiltonian H_S is given by

$$H_S = \sum_{i=1}^{m} \left(\frac{\hbar}{2} \epsilon_i \sigma_z^i + \hbar \Delta_i \sigma_x^i \right) \ . \tag{2}$$

Here σ_z and σ_x are the usual Pauli spin matrices, m denotes the number of two-level systems, ϵ_i represents the energy difference between states $|i-1\rangle$ and $|i\rangle$ and Δ_i is the tunnelling frequency between the ith and $(i-1)$th BChla sites.

The bath is modelled as a set of harmonic oscillators and the relevant Hamiltonian can be written as

$$H_B = \sum_k \hbar \omega_k b_k^\dagger b_k \ , \tag{3}$$

where b_k and $b_k^\dagger$ are the annihilation and the creation operators for the k^{th} mode, respectively.

At present, there is no direct experimental method to get accurate information about the interaction of phonon modes (same or different) with the BChla sites in FMO complex. The fluctuations in the site energies of different BChla sites may be uncorrelated if different BChla sites couple to different phonon modes[36]. Based on this assumption, efforts with uncorrelated fluctuations have been made by a number of authors with[35–42]. Considering the different bath modes for the different BChla sites, the standard spin-boson interaction can be described by the following Hamiltonian:

$$H_{SB} = \sum_{i=1}^{m} \sum_k \frac{\hbar}{2} \sigma_z^i g_{ik} (b_{ik} + b_{ik}^\dagger) \ . \tag{4}$$

where g_{ik} is the coupling constant between the ith two-level system and the kth bath mode.

On the other hand, if all the BChla sites couple to the same phonon mode, the fluctuations in the site energies may be correlated[36]. On the basis of conjecture of correlated fluctuations[49,50], several theoretical models have been proposed for the same phonon mode for all the BChla sites in FMO complex[43–46,51]. The standard spin-boson interaction Hamiltonian with the assumption of same phonon mode for all the BChla sites, can be written as

$$H_{SB} = \sum_{i=1}^{m} \left(\frac{\hbar}{2} \sigma_z^i \sum_k g_{ik} (b_k + b_k^\dagger) \right) \ . \tag{5}$$

Using the above Hamiltonian in equation 1, the time-evolution of the density matrix of the FMO complex can be described by the following master equation in Schrodinger picture[52,53]:

$$\begin{aligned} \dot{\rho} \ &= \ -\tfrac{i}{\hbar} [H_S, \rho] \\ &+ \ \tfrac{1}{4} \sum_{i,j}^{m} \left\{ \left(\sigma_z^j \rho \sigma_z^i - \rho \sigma_z^i \sigma_z^j \right) D_{K_i K_j}(t) \right. \\ &+ \ \left(\sigma_z^j \rho \sigma_z^i - \sigma_z^i \sigma_z^j \rho \right) D^*_{K_i K_j}(t) \\ &+ \ \left(\sigma_z^i \rho \sigma_z^j - \sigma_z^j \sigma_z^i \rho \right) U_{K_i K_j}(t) \\ &+ \ \left. \left(\sigma_z^i \rho \sigma_z^j - \rho \sigma_z^j \sigma_z^i \right) U^*_{K_i K_j}(t) \right\} \ . \end{aligned} \tag{6}$$

The time-dependent coefficients, which contain the information about system-reservoir correlation, render the equation non-Markovian and are given by

$$D_{K_i K_j}(t) = \int_0^t dt' \int_0^\infty d\omega J_{K_i K_j}(\omega) \bar{n}(\omega, T) e^{-i\omega(t-t')} \ , \tag{7}$$

$$U_{K_i K_j}(t) = \int_0^t dt' \int_0^\infty d\omega J_{K_i K_j}(\omega) [\bar{n}(\omega, T) + 1] e^{-i\omega(t-t')} \ , \tag{8}$$

where

$$\bar{n}(\omega, T) = \frac{1}{e^{\frac{\hbar\omega}{K_B T}} - 1}$$

is the average number of phonons for a harmonic oscillator with the frequency between ω and $\omega + d\omega$ in the thermal equilibrium at temperature T. $J_{K_i K_j}(\omega)$ is the spectral density which contains the information about frequencies of the bath modes and the coupling of these bath modes with system. For electron transfer reactions in FMO complex, it is convenient to use Ohmic spectral density[21,43,48]. We use[43,54,55] the form of this spectral density as

$$J_{K_i K_j}(\omega) = 2K_{i,j}\omega \left(\frac{\omega}{\omega_{c_{i,j}}}\right)^{(s-1)} e^{-\omega/\omega_{c_{i,j}}} \ ,$$

where $\omega_{c_{i,j}}$ is the corresponding cut-off frequency, $K_{i,j} = \sqrt{K_i K_j}$, $K_i = g_{ik}^2$ and we choose $s = 1$, corresponding to Ohmic spectral density. Note that the reorganisation energy λ, for Ohmic spectrum, is related to the damping strength $K_{i,j}$ as[54].

$$\lambda_{i,j} = 2K_{i,j}\omega_{c_{i,j}} \ . \tag{9}$$

III. PATHWAYS OF EET DYNAMICS

As the FMO complex is a trimer with identical subunits, the coupling between BChla's of two different monomeric subunits is small, the decay of coherence between them due the environmental de-phasing is very rapid[22]. Hence inter-subunit coupling is assumed to very small and the EET is considered within one subunit[36]. On the basis of theoretical prediction[22] and experimental observation[56], the spatial distribution of BChla's inside the monomeric subunits of FMO complex is known. Inside a monomeric subunit, BChla's are oriented in such a manner that BChla 1 and BChla 6 are close to the chlorosome antenna and BChla 3 and BChla 4 are close to the reaction centre. The absorption of the baseplate BChla in FMO complex of *Chlorobium tepidum* occurs at an energy 12500 cm^{-1}, which lies between the site energies of BChla 1 (12410 cm^{-1}) and BChla 6 (12630 cm^{-1})[22,57,58]. So any excitation energy which is absorbed by the baseplate BChla of the chlorosome antenna, will be shared between the BChla 1 and BChla 6. Then through the pathways, suitably optimised in order to minimise the loss, this excitation energy will reach the BChla 3 or BChla 4, thereafter to be harvested by the reaction centre. Theoretical calculation of excitonic coupling indicates that there are *two* pathways[22] which are further confirmed by Brixner et al. with 2D electronic spectroscopy[59,60]. Below, we study the EET through these two pathways.

A. The First Pathway

Although the FMO complex has two BChla sites to receive the excitation energy from baseplate, the lower value of the site energy of BChla 1 as compared to the baseplate BChla (as shown in figure 2) makes it easy for BChla 1 to get excitation energy. On the basis of excitonic coupling between different sites as given by Adolphs and Renger[22], it is assumed that excitation at BChla 1 will be transferred to BChla 2 and BChla 6. The relevant pathway is displayed in the figure 2.

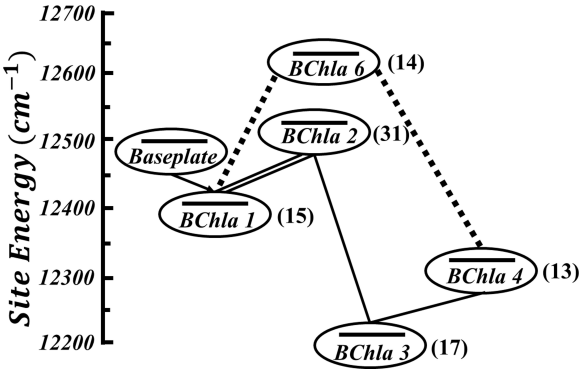

FIG. 2: Site energies of Bchla's in the monomer of FMO complex and the first pathway of excitation energy transfer. Double line indicate strong pigment-pigment coupling($\Delta > 60cm^{-1}$), single line indicate medium pigment-pigment coupling ($30cm^{-1} < \Delta < 60cm^{-1}$) and dashed line implies weak pigment-pigment coupling $\Delta < 30cm^{-1}$). Values in the parentheses are local environmental reorganization energies.

The oscillations of excitation in FMO complex, as experimentally observed, implies adiabatic electron transfer. Electron transfer dynamics occurs in the *adiabatic limit*[54], defined by

$$\frac{2\Delta_i}{\omega_{c_{i,j}}} \geq 1 \ . \tag{10}$$

It is evident from equations 9 and 10 that in the *adiabatic limit*, pigment-pigment coupling Δ_i is inversely proportional to the pigment-protein coupling $K_{i,j}$. So if two BChla sites couple strongly with each other, they couple weakly with the environment and vice-versa.

1. Different Bath Modes

In the case of interaction of different BChla sites with different bath modes, the cross terms $K_{i,j}$ $(i \neq j)$ are not relevant, reflecting the consideration that the bath modes, local to each BChla site are not correlated to each other. This simplifies the master equation (6), in which the the sum over i and j reduce to sum over the index

i only. In the table I, the relevant non-zero pigment-protein coupling terms are displayed. Note that in this case, we use[43]

$$\frac{2\Delta_i}{\omega_{c_{i,j}}} = 1.052\ . \tag{11}$$

Different values of pigment-protein couplings and cut-off frequencies are obtained (see the Table I) by using equations 9 and 11, where we choose the same re-organisation energy for all the BChla sites as used by Fleming et. al.[36] ($\lambda = 35\ \mathrm{cm}^{-1}$), in order to compare our results.

TABLE I: Parameters used to simulate the first pathway, when different BChla sites interact with different phonon modes. Same re-organization energy is used for all BChla sites.

Pigment-protein couplings	Cut-off frequencies (in cm^{-1})
$K_{1,1} = 0.1050$	$\omega_{c_{1,1}} = 166.7265$
$K_{2,2} = 0.2989$	$\omega_{c_{2,2}} = 058.5539$
$K_{3,3} = 0.1721$	$\omega_{c_{3,3}} = 101.7089$
$K_{4,4} = 0.6719$	$\omega_{c_{4,4}} = 026.0451$
$K_{5,5} = 0.5415$	$\omega_{c_{5,5}} = 032.3187$

We solve the non-Markovian master equation 6 and simulate the population dynamics. In figure 3, we show the temporal evolution of the occupation probability of the sites along the first pathway at cryogenic temperature 77 K. With the use of different values of pigment-protein couplings for the initial excitation to BChla 1 (dashed curves in figure 3), we observe the time scale for which the oscillations of excitation exist is about 425 fs, less than experimental findings[19]. It suggests that the coupling to different phonon modes gives rise to the shorter oscillatory time-scales and the uncorrelated fluctuations are not therefore able to preserve oscillations of excitation for the time-scale observed in experiment[19].

Generally, the experimentally observed EET dynamics refers to a model that assumes all the BChla sites to have the homogeneous local environment[36]. In order to compare our results with this over-simplified model, we assume that all the BChla sites couple to the same pigment-protein coupling $K = 0.105$ (corresponding to a phonon relaxation time $\tau_c = 50$ fs) and study the EET dynamics using equation 6 (solid curve in figure 3). We observe that the time-scale of oscillations of EET is of the order of 600 fs, which is closely matching with the results obtained by Ishizaki *et. al.*[36]. Hence the over-simplified treatment of this kind, based on the contradictory assumption of homogeneous protein environment around all the BChla sites, reveals long-lasting oscillations even with uncorrelated fluctuations. While in the real situation of inhomogeneous protein environment, uncorrelated fluctuations give short time-scale of oscillations, as shown by the dashed curves in figure 3. Therefore, as obvious

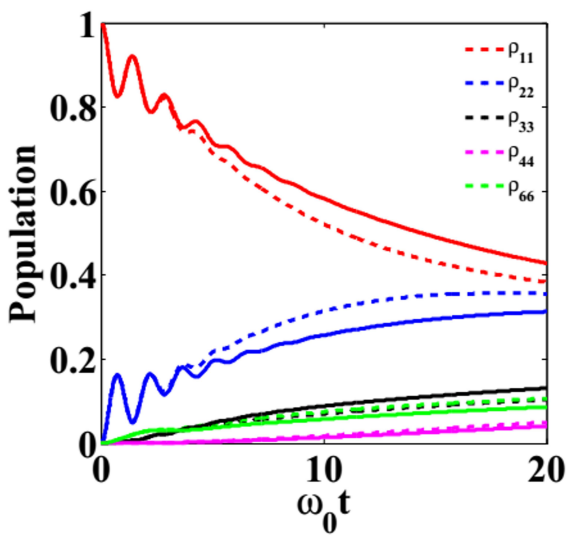

FIG. 3: (Color online) Excitation energy transfer dynamics of the first pathway at cryogenic temperature T = 77 K, when different BChla sites interact with different phonon modes. Dashed curves give EET dynamics computed using different values of pigment-protein couplings for different BChla sites. Solid curves refer to the population dynamics obtained using same value of pigment-protein coupling for all the BChla sites. We choose $\omega_0 = 100\ \mathrm{cm}^{-1}$ for normalization.

from the above study, one needs to consider the correlated bath fluctuations, to correctly mimic the realistic situation of inhomogeneous protein environment, which we will study in the following.

2. Common Bath Modes

Assuming the coupling of all the BChla sites with the same bath mode, different values of pigment-protein couplings and cut-off frequencies are obtained (see the Table II) by using equations 9 and

$$\frac{2\Delta_i}{\omega_{c_{i,j}}} = 1\ . \tag{12}$$

In order to consider the environmental asymmetry around different BChla site, we consider different values of re-organization energies for different BChla sites following Coker et. al.[47] (see figure 2).

Again the non-Markovian master equation 6 is solved to study quantum dynamics using the different pigment-protein couplings of the Table II.

Temporal evolution of excitation energy along the first pathway is shown in figure 4 for different temperatures. Considering only the BChla 1 to be populated initially, one obtains a large-amplitude population oscillations between BChla 1 and BChla 2, which exist for 650 fs at

TABLE II: Parameters used to simulate the first pathway, when all BChla sites interact with same phonon mode. Different values of re-organization energies are used for different BChla sites.

Pigment-protein couplings	Cut-off frequencies (in cm^{-1})
$K_{1,1} = 0.0656$	$\omega_{c_{1,1}} = 175.4000$
$K_{2,2} = 0.1948$	$\omega_{c_{2,2}} = 061.6000$
$K_{3,3} = 0.0701$	$\omega_{c_{3,3}} = 107.0000$
$K_{4,4} = 0.2646$	$\omega_{c_{4,4}} = 027.4000$
$K_{5,5} = 0.1985$	$\omega_{c_{5,5}} = 034.0000$
$K_{2,1} = 0.1130$	$\omega_{c_{2,1}} = 103.9823$
$K_{3,2} = 0.1169$	$\omega_{c_{3,2}} = 083.4046$
$K_{3,1} = 0.0678$	$\omega_{c_{3,1}} = 140.1180$
$K_{4,3} = 0.1362$	$\omega_{c_{4,3}} = 054.1483$
$K_{4,2} = 0.2270$	$\omega_{c_{4,2}} = 042.4009$
$K_{4,1} = 0.1317$	$\omega_{c_{4,1}} = 071.1845$
$K_{5,4} = 0.2292$	$\omega_{c_{5,4}} = 030.5410$
$K_{5,3} = 0.1180$	$\omega_{c_{5,3}} = 060.3814$
$K_{5,2} = 0.1966$	$\omega_{c_{5,2}} = 047.6857$
$K_{5,1} = 0.1141$	$\omega_{c_{5,1}} = 079.9737$

a cryogenic temperature $T = 77$ K and last for more than 300 fs at room temperature $T = 277$ K, which are in conformity with the experimental results[19,20]. Our dynamical studies show that correlated fluctuations preserve the oscillations of excitation for long time and provide the same time-scale of oscillations observed in experiments[19,20]. It reveals that local protein environment, which we mimic by different values of pigment-protein couplings, show us more accurate mechanism of EET in which correlated fluctuations play an important role. To check the dynamics of EET along second pathway, we will consider the coupling to the same phonon mode only.

Further, a large-amplitude population oscillation between BChla 1 and BChla 2 exists for the longest time. As the tunneling frequency between BChla 1 and BChla 2 is highest, so they interact very strongly with each other. Now in the *adiabatic limit* of excitation transfer, if two BChla sites interact very strongly with each other, their interaction with the environment becomes weak and vice-versa. Hence the de-phasing and dissipation due to environment becomes very weak, leading to large amplitude oscillations of excitation between BChla 1 and BChla 2 persisting for long times. We observe a small-amplitude oscillatory dynamics of populations in BChla 3 and BChla 4.

We also observed that the pigment-pigment coupling plays the major role in selecting the pathway, sometimes overshadowing the role of the BChla site energy. For example, although the site energy of BChla 2 is more than that of BChla 1, population moves from BChla 1 to BChla 2 due to large pigment-pigment coupling between them. We find that this kind of uphill migration, the transfer of excitation from low energy site to high energy site, delays the excitation energy transfer process and hence the robustness. Moreover, the selection of pathways is totally independent from pigment-protein coupling and protein environment as has been observed in earlier works also[22,35,36].

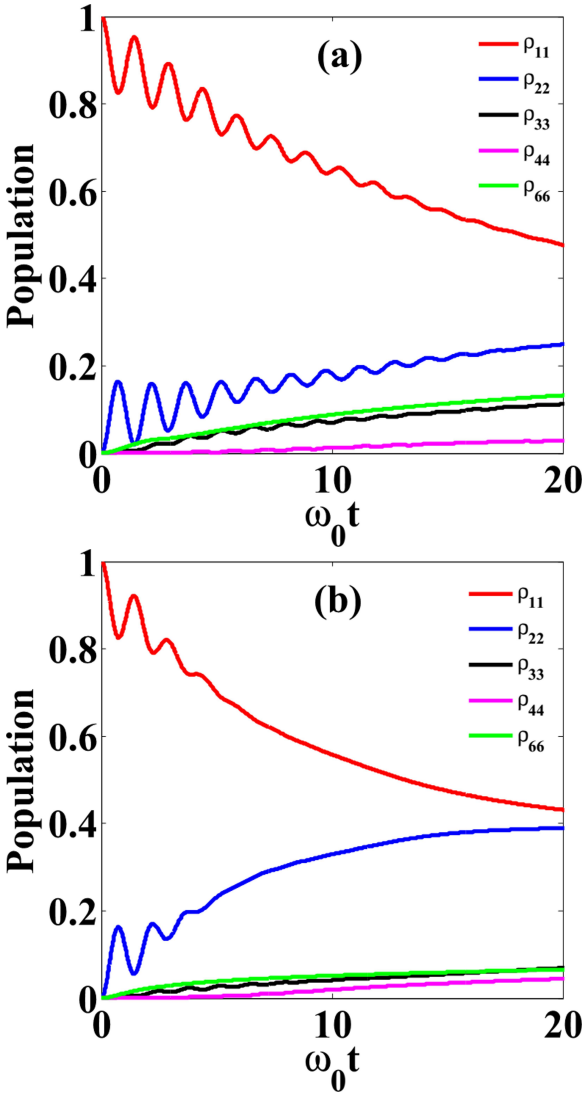

FIG. 4: (Color online) Excitation energy transfer dynamics of the first pathway at cryogenic temperature T = 77 K [(a)] and at room temperature T = 277 K [(b)], when all BChla sites interact with identical phonon mode.

B. The Second Pathway

A large value of the site energy of BChla 6 as compared to the baseplate BChla (as evident from figure 5) requires more attention to convey electronic excitation energy through BChla 6. According to the detailed balance condition between BChla 6 and the baseplate BChla, if the de-excitation of BChla 6 were long lasting, the excitation could easily come back to the baseplate BChla. To get rid from this backward excitation

transfer, BChla 6 needs to transfer its excitation to other BChla's as quickly as possible[36]. This condition is satisfied by having BChla 6 be strongly coupled to BChla 4, BChla 5 and BChla 7. Both BChla 5 and BChla 7 are also strongly coupled to BChla 4 and BChla 4 is strongly coupled to BChla 3. We consider this as the second pathway.

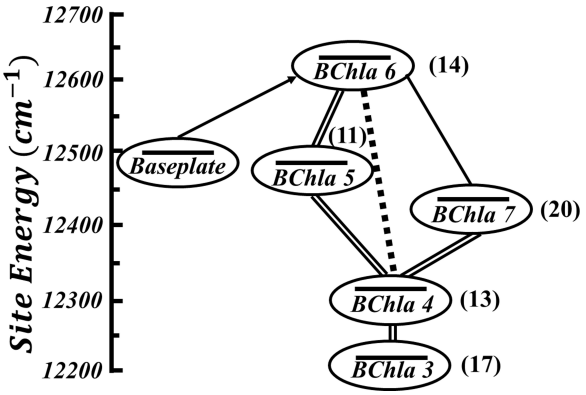

FIG. 5: Site energies of Bchla's in the monomer of FMO complex and second pathway of excitation energy transfer.

Again in the *adiabatic limit* of EET, and considering the coupling to same phonon mode, the pigment-protein couplings and the cut-off frequencies are calculated (with the different values of re-organization energies, see figure 5) from equations 9 and 12 for the second pathway and are listed in the Table III.

The time-dependent occupation probabilities of different BChla sites of the second pathway are shown in figure 6, assuming the BChla 6 is initially populated. It is evident that excitation energy is quickly distributed between all the levels, which indicates fast de-localization of the excitation energy over all the BChla sites of the second pathway irrespective of the temperature. As the site energies of all the BChla sites of second pathway are less than the linker pigment BChla 6, so the downhill migration (transfer of excitation from high energy site to low energy site) increases the robustness of this pathway. Interestingly, the times of oscillation of excitation are little less as compared to the first pathway at all temperatures. As all the pigment-pigment couplings of second pathway are less as compared to pigment-pigment coupling between BChla 1 and BChla 2, again in the *adiabatic limit*, they interact strongly with environment, hence time-scale of oscillation is less. Moreover we observe that for both the pathways, the amplitude of oscillations increases with increase in pigment-pigment coupling and with decrease in temperature, while the frequency of oscillations remains independent of both these parameters.

TABLE III: Parameters used to simulate the second pathway, when all BChla sites interact with identical phonon mode. Different values of re-organization energies are used for different BChla sites.

Pigment-protein couplings	Cut-off frequencies (in cm^{-1})
$K_{1,1} = 0.0385$	$\omega_{c_{1,1}} = 162.2000$
$K_{2,2} = 0.1071$	$\omega_{c_{2,2}} = 079.4000$
$K_{3,3} = 0.1985$	$\omega_{c_{3,3}} = 034.0000$
$K_{4,4} = 0.0426$	$\omega_{c_{4,4}} = 141.0000$
$K_{5,5} = 0.0652$	$\omega_{c_{5,5}} = 126.6000$
$K_{6,6} = 0.0701$	$\omega_{c_{6,6}} = 107.0000$
$K_{2,1} = 0.0642$	$\omega_{c_{2,1}} = 114.8754$
$K_{3,2} = 0.1458$	$\omega_{c_{3,2}} = 052.2977$
$K_{3,1} = 0.0874$	$\omega_{c_{3,1}} = 074.3707$
$K_{4,3} = 0.0920$	$\omega_{c_{4,3}} = 069.2935$
$K_{4,2} = 0.0675$	$\omega_{c_{4,2}} = 107.4074$
$K_{4,1} = 0.0405$	$\omega_{c_{4,1}} = 151.2346$
$K_{5,4} = 0.0527$	$\omega_{c_{5,4}} = 135.1992$
$K_{5,3} = 0.1138$	$\omega_{c_{5,3}} = 065.9051$
$K_{5,2} = 0.0836$	$\omega_{c_{5,2}} = 100.1794$
$K_{5,1} = 0.0501$	$\omega_{c_{5,1}} = 144.7106$
$K_{6,5} = 0.0676$	$\omega_{c_{6,5}} = 116.4941$
$K_{6,4} = 0.0546$	$\omega_{c_{6,4}} = 123.6264$
$K_{6,3} = 0.1180$	$\omega_{c_{6,3}} = 060.3814$
$K_{6,2} = 0.0866$	$\omega_{c_{6,2}} = 092.3788$
$K_{6,1} = 0.0520$	$\omega_{c_{6,1}} = 132.2115$

IV. CONCLUSIONS

In conclusions, we study the temporal and spatial dynamics of EET, by employing a non-Markovian master equation. We demonstrate the sensitivity of EET dynamics in FMO complex to the difference in local protein environment around different BChla sites. We have found that the time scale for excitation oscillation as observed in the experiments can be modelled either by using the same pigment-protein coupling constant with local bath modes or by using different pigment-protein coupling constants with the common bath modes. As the local protein environment of different pigment sites are different, we emphasize the use of common bath modes with different coupling constants. This further illustrates the importance of correlated fluctuations, predicted previously. Dynamical simulation, in real protein environment, suggest that large amplitude oscillations of excitation persist between those BChla sites which have weak coupling with the environment. Due to inhomogeneous environment, each BChla site has different pigment-protein coupling, hence time-scales of oscillation are different for different BChla sites. These differences in the oscillatory time-scales of individual BChla site should be observable, by changing dissipative characteristics of local environment around different BChla sites. Further, we have shown that the downhill migration of excitation increase the robustness of EET dynamics. This indicates a new flowchart of excitation energy transfer - the pathway without any energetic minima should be more robust

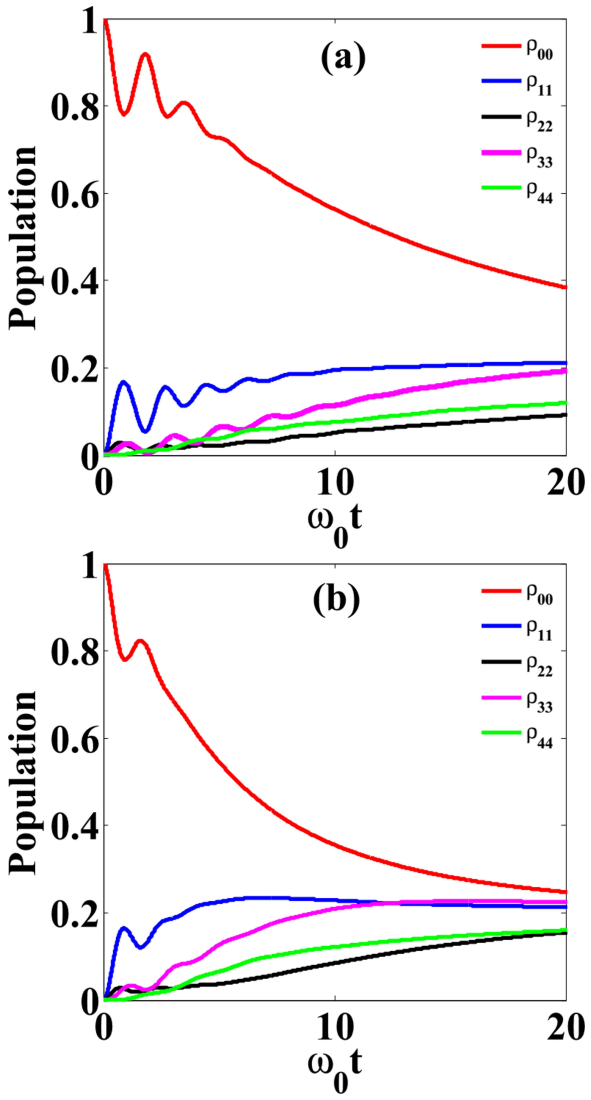

FIG. 6: (Color online) Excitation energy transfer dynamics on the second pathway at cryogenic temperature $T = 77$ K [(a)] and at room temperature $T = 277$ K [(b)], when all BChla sites interact with same phonon mode.

as compared to the pathway with energetic minima.

ACKNOWLEDGMENTS

One of us (D.S.) gratefully acknowledges the financial support from the Department of Science and Technology (DST), Govt. of India, under the grant number SR/S2/LOP-0021/2012.

[1] R. E. Blankenship, *Molecular Mechanism of Photosynthesis* (World Scientific, London, 2002).
[2] N. Campbell and J. Reece, *Biology* (Benjamin-Cummings, San Francisco, 2005).
[3] G. J. Meyer, "Chemists quest for inexpensive, efficient, and stable photovoltaics," J.Phys. Chem. Lett. **2**, 1965–1966 (2011).
[4] D. Gust, T. A. Moore, and A. L. Moore, "Solar fuels via artificial photosynthesis," Acc. Chem. Res. **42**, 1890–1898 (2009).
[5] K. Maeda and K. Domen, "Photocatalytic water splitting: Recent progress and future challenges," J.Phys. Chem. Lett. **1**, 2655–2661 (2010).
[6] T. E. Mallouk, "The emerging technology of solar fuels," J.Phys. Chem. Lett. **1**, 2738–2739 (2010).
[7] V. I. Vullev, "From biomimesis to bioinspiration: Whats the benefit for solar energy conversion applications?" J.Phys. Chem. Lett. **2**, 503–508 (2011).
[8] D. Gust, T. A. Moore, and A. L. Moore, "Mimicking photosynthetic solar energy transduction," Acc. Chem. Res. **34**, 40–48 (2001).
[9] H. V. Amerongen, L. Valkunas, and R. Grondelle, *Photosynthetic Excitons* (World Scientific, Singapore, 2000).
[10] Y.-C. Cheng and G. R. Fleming, "Dynamics of light harvesting in photosynthesis," Ann. Rev. Phys. Chem. **60**, 241–262 (2009).
[11] G. D. Scholes, G. R. Fleming, A. Olaya-Castro, and R. van Grondelle, "Lessons from nature about solar light harvesting," Nature Chemistry **3**, 763–774 (2011).
[12] V. I. Novoderezhkin and R. van Grondelle, "Physical origins and models of energy transfer in photosynthetic light-harvesting," Phys. Chem. Chem. Phys. **12**, 7352–7365 (2010).
[13] R. Fenna, B. Matthews, J. Olson, and E. Shaw, "Structure of a bacteriochlorophyll-protein from the green photosynthetic bacterium chlorobium limicola: Crystallographic evidence for a trimer," J. Mol. Biol. **84**, 231 – 240 (1974).
[14] R. E. Fenna and B. W. Matthews, "Chlorophyll arrangement in a bacteriochlorophyll protein from chlorobium limicola," Nature **258**, 573–577 (1975).
[15] A. Camara-Artigas, R. E. Blankenship, and J. P. Allen, "The structure of the fmo protein from chlorobium tepidum at 2.2 resolution," Photosynth. Res. **75**, 49–55 (2003).
[16] M. Sarovar, A. Ishizaki, G. R. Fleming, and K. B. Whaley, "Quantum entanglement in photosynthetic light-harvesting complexes," Nature Physics **6**, 462–467 (2010).
[17] T. Brixner, T. Mancal, I. V. Stiopkin, and G. R. Fleming, "Phase-stabilized two-dimensional electronic spectroscopy," J. Chem. Phys. **121**, 4221–4236 (2004).
[18] G. S. Schlau-Cohen, A. Ishizaki, and G. R. Fleming, "Two-dimensional electronic spectroscopy and photosynthesis: Fundamentals and applications to photosynthetic light-harvesting," Chem. Phys. **386**, 1 – 22 (2011).
[19] G. S. Engel, T. R. Calhoun, E. L. Read, T.-K. Ahn, T. Mancal, Y.-C. Cheng, R. E. Blankenship, and G. R. Fleming, "Evidence for wavelike energy transfer through quantum coherence in photosynthetic systems," Nature **446**, 782–786 (2007).
[20] G. Panitchayangkoon, D. Hayes, K. A. Fransted, J. R. Caram, E. Harel, J. Wen, R. E. Blankenship, and G. S. Engel, "Long-lived quantum coherence in photosynthetic complexes at physiological temperature," PNAS **107**, 12766–12770 (2010).
[21] O. K. V. May, *Charge and energy transfer dynamics in molecular systems* (Wiley-VCH, 2010).
[22] J. Adolphs and T. Renger, "How proteins trigger excitation energy transfer in the fmo complex of green sulfur bacteria," Biophys. J. **91**, 2778–2797 (2006).
[23] M. Mohseni, P. Rebentrost, S. Lloyd, and A. Aspuru-Guzik, "Environment-assisted quantum walks in photosynthetic energy transfer," J. Chem.l Phys. **129**, 174106 (2008).
[24] B. Palmieri, D. Abramavicius, and S. Mukamel, "Lindblad equations for strongly coupled populations and coherences in photosynthetic complexes," J. Chem. Phys. **130**, 204512 (2009).
[25] F. Caruso, A. W. Chin, A. Datta, S. F. Huelga, and M. B. Plenio, "Highly efficient energy excitation transfer in light-harvesting complexes: The fundamental role of noise-assisted transport," J. Chem. Phys. **131**, 105106 (2009).
[26] L. A. Baker and S. Habershon, "Robustness, efficiency, and optimality in the Fenna-Matthews-Olson photosynthetic pigment-protein complex," J. Chem. Phys. **143**, 105101 (2015).

[27] J. Prior, A. W. Chin, S. F. Huelga, and M. B. Plenio, "Efficient simulation of strong system-environment interactions," Phys. Rev. Lett. **105**, 050404 (2010).

[28] S. Hoyer, A. Ishizaki, and K. B. Whaley, "Spatial propagation of excitonic coherence enables ratcheted energy transfer," Phys. Rev. E **86**, 041911 (2012).

[29] M. Sarovar, Y.-C. Cheng, and K. B. Whaley, "Environmental correlation effects on excitation energy transfer in photosynthetic light harvesting," Phys. Rev. E **83**, 011906 (2011).

[30] G.-Y. Chen, N. Lambert, C.-M. Li, Y.-N. Chen, and F. Nori, "Rerouting excitation transfers in the fenna-matthews-olson complex," Phys. Rev. E **88**, 032120 (2013).

[31] S. Hoyer, M. Sarovar, and K. B. Whaley, "Limits of quantum speedup in photosynthetic light harvesting," New J. Phys. **12**, 065041 (2010).

[32] J. Wu, F. Liu, Y. Shen, J. Cao, and R. J. Silbey, "Efficient energy transfer in light-harvesting systems, I: optimal temperature, reorganization energy and spatialtemporal correlations," New J. Phys. **12**, 105012 (2010).

[33] P. Rebentrost, M. Mohseni, and A. Aspuru-Guzik, "Role of quantum coherence and environmental fluctuations in chromophoric energy transport," J. Phys. Chem. B **113**, 9942–9947 (2009).

[34] C. G. Gillis and G. A. Jones, "A theoretical investigation into the effects of temperature on spatiotemporal dynamics of eet in the fmo complex," J. Phys. Chem. B **119**, 4165–4174 (2015).

[35] J. Zhu, S. Kais, P. Rebentrost, and A. Aspuru-Guzik, "Modified scaled hierarchical equation of motion approach for the study of quantum coherence in photosynthetic complexes," J.Phys. Chem. B **115**, 1531–1537 (2011).

[36] A. Ishizaki and G. R. Fleming, "Theoretical examination of quantum coherence in a photosynthetic system at physiological temperature," PNAS **106**, 17255–17260 (2009).

[37] P. Nalbach, D. Braun, and M. Thorwart, "Exciton transfer dynamics and quantumness of energy transfer in the fenna-matthews-olson complex," Phys. Rev. E **84**, 041926 (2011).

[38] G. Ritschel, J. Roden, W. T. Strunz, and A. Eisfeld, "An efficient method to calculate excitation energy transfer in light-harvesting systems: application to the fennamatthewsolson complex," New J. Phys. **13**, 113034 (2011).

[39] P. Bhattacharyya and K. L. Sebastian, "Adiabatic eigenfunction-based approach for coherent excitation transfer: An almost analytical treatment of the fenna-matthews-olson complex," Phys. Rev. E **87**, 062712 (2013).

[40] C. A. Mujica-Martinez, P. Nalbach, and M. Thorwart, "Quantification of non-markovian effects in the fenna-matthews-olson complex," Phys. Rev. E **88**, 062719 (2013).

[41] A. Shabani, M. Mohseni, H. Rabitz, and S. Lloyd, "Efficient estimation of energy transfer efficiency in light-harvesting complexes," Phys. Rev. E **86**, 011915 (2012).

[42] X. Chen and R. J. Silbey, "Excitation energy transfer in a non-markovian dynamical disordered environment: Localization, narrowing, and transfer efficiency," J. Phys. Chem. B **115**, 5499–5509 (2011).

[43] L. A. Pachon and P. Brumer, "Physical basis for long-lived electronic coherence in photosynthetic light-harvesting systems," J.Physl Chem. Lett. **2**, 2728–2732 (2011).

[44] A. W. Chin, J. Prior, R. Rosenbach, F. Caycedo-Soler, S. F. Huelga, and M. B. Plenio, "The role of non-equilibrium vibrational structures in electronic coherence and recoherence in pigment-protein complexes," Nat Phys **9**, 113–118 (2013).

[45] A. W. Chin, A. Datta, F. Caruso, S. F. Huelga, and M. B. Plenio, "Noise-assisted energy transfer in quantum networks and light-harvesting complexes," New J. Phys. **12**, 065002 (2010).

[46] P. Nalbach, J. Eckel, and M. Thorwart, "Quantum coherent biomolecular energy transfer with spatially correlated fluctuations," New J. Phys. **12**, 065043 (2010).

[47] E. Rivera, D. Montemayor, M. Masia, and D. F. Coker, "Influence of site-dependent pigmentprotein interactions on excitation energy transfer in photosynthetic light harvesting," J. Phys. Chem. B **117**, 5510–5521 (2013).

[48] J. B. Gilmore and R. H. McKenzie, "Criteria for quantum coherent transfer of excitations between chromophores in a polar solvent," Chem. Phys. Lett. **421**, 266 – 271 (2006).

[49] H. Lee, Y.-C. Cheng, and G. R. Fleming, "Coherence dynamics in photosynthesis: Protein protection of excitonic coherence," Science **316**, 1462–1465 (2007).

[50] H. Treutlein, K. Schulten, A. T. Brunger, M. Karplus, J. Deisenhofer, and H. Michel, "Chromophore-protein interactions and the function of the photosynthetic reaction center: a molecular dynamics study," PNAS **89**, 75–79 (1992).

[51] L. Yang, D. Abramavicius, and S. Mukamel, "Signatures of three-exciton correlations in the coherent and incoherent nonlinear optical response of photosynthetic complexes," New J. Phys. **12**, 065046 (2010).

[52] H. J. Carmichael, *Statistical Methods in Quantum optics 1* (Springer, 2002).

[53] M. M. Ali, P.-W. Chen, and H.-S. Goan, "Decoherence-free subspace and disentanglement dynamics for two qubits in a common non-markovian squeezed reservoir," Phys. Rev. A **82**, 022103 (2010).

[54] U. Weiss, *Quantum dissipative systems* (World Scientific, Singapore, 2008).

[55] W.-M. Zhang, P.-Y. Lo, H.-N. Xiong, M. W.-Y. Tu, and F. Nori, "General non-markovian dynamics of open quantum systems," Phys. Rev. Lett. **109**, 170402 (2012).

[56] J. Wen, H. Zhang, M. L. Gross, and R. E. Blankenship, "Membrane orientation of the fmo antenna protein from chlorobaculum tepidum as determined by mass spectrometry-based footprinting," PNAS **106**, 6134–6139 (2009).

[57] C. Francke and J. Amesz, "Isolation and pigment composition of the antenna system of four species of green sulfur bacteria," Photosynth. Res. **52**, 137–146 (1997).

[58] N.-U. Frigaard, H. Li, P. Martinsson, S. K. Das, H. A. Frank, T. J. Aartsma, and D. A. Bryant, "Isolation and characterization of carotenosomes from a bacteriochlorophyll c-less mutant of chlorobium tepidum," Photosynth. Res. **86**, 101–11 (2005).

[59] T. Brixner, J. Stenger, H. M. Vaswani, M. Cho, R. E. Blankenship, and G. R. Fleming, "Two-dimensional spectroscopy of electronic couplings in photosynthesis," Nature **434**, 625–628 (2005).

[60] M. Cho, H. M. Vaswani, T. Brixner, J. Stenger, and G. R. Fleming, "Exciton analysis in 2d electronic spectroscopy," J.Phys. Chem. B **109**, 10542–10556 (2005).